Supporting Information

A Near Infrared-Peptide Probe with Tumor-Specific Excretion Retarded Effect for Image-Guided Surgery of Renal Cell Carcinoma

Hong-Wei An,[‡,⊥,∥] Dayong Hou,[†,‡,§,∥] Rui Zheng,[‡] Man-Di Wang,[‡] Xiang-Zhong Zeng,[‡] Wu-Yi Xiao,[‡] Tong-Da Yan,[‡] Jia-Qi Wang,[†,‡,§] Chang-Hao Zhao,[†,‡,§] Li-Ming Cheng,[†,§] Jin-Ming Zhang,[†,§] Lu Wang,[†,§] Zi-Qi Wang,[*,†,‡,§] Hao Wang[*,‡,§] and Wanhai Xu[*,†,§]

[†]Department of Urology, the Fourth Hospital of Harbin Medical University, Heilongjiang Key Laboratory of Scientific Research in Urology, Harbin, 150001, China.

[‡]CAS Key Laboratory for Biomedical Effects of Nanomaterials and Nanosafety, CAS Center for Excellence in Nanoscience, National Center for Nanoscience and Technology (NCNST), Beijing, 100190, China

[§]NHC Key Laboratory of Molecular Probes and Targeted Diagnosis and Therapy, Harbin, 150001, China.

[⊥] CAS Key Laboratory for Biomedical Effects of Nanomaterials and Nanosafety, Institute of High Energy Physics, Yuquan Road, Beijing, 100049, China

KEYWORDS: self-assembly, supramolecular, probe, renal cell carcinoma, image-guided surgery

E-mail: xuwanhai@hrbmu.edu.cn, wanghao@nanoctr.cn, wangziqi@hrbmu.edu.cn.

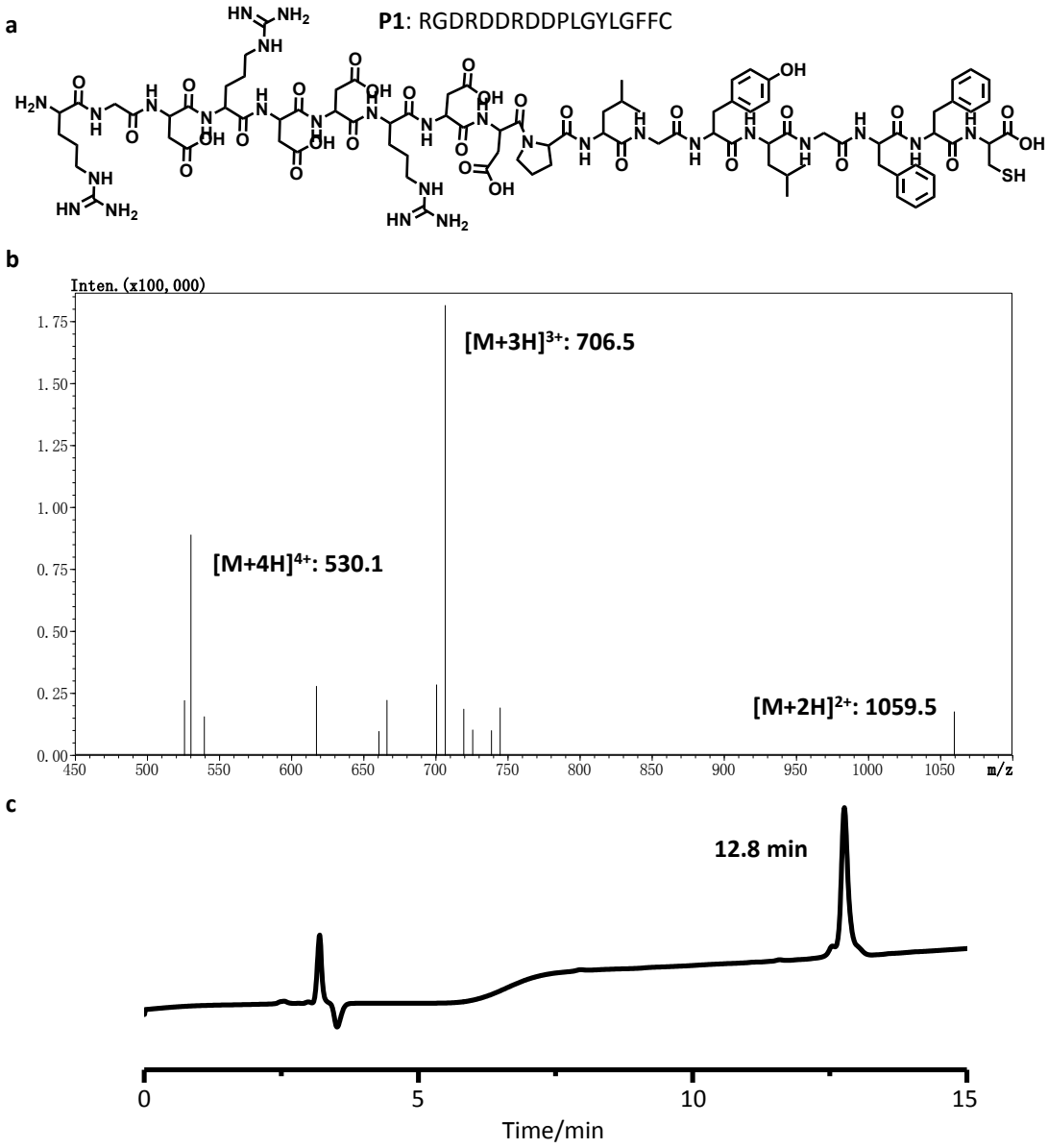

Scheme S1. (a) The structure of P1; (b) MS-ESI and (c) HPLC spectra of P1. The method of HPLC spectra was as follows: solvent A, 0.1% trifluoroacetic in 100% water; solvent B, 0.1% trifluoroacetic in 100% acetonitrile; 0.01 min, 25% solvent B, 15 min, 60% solvent B.

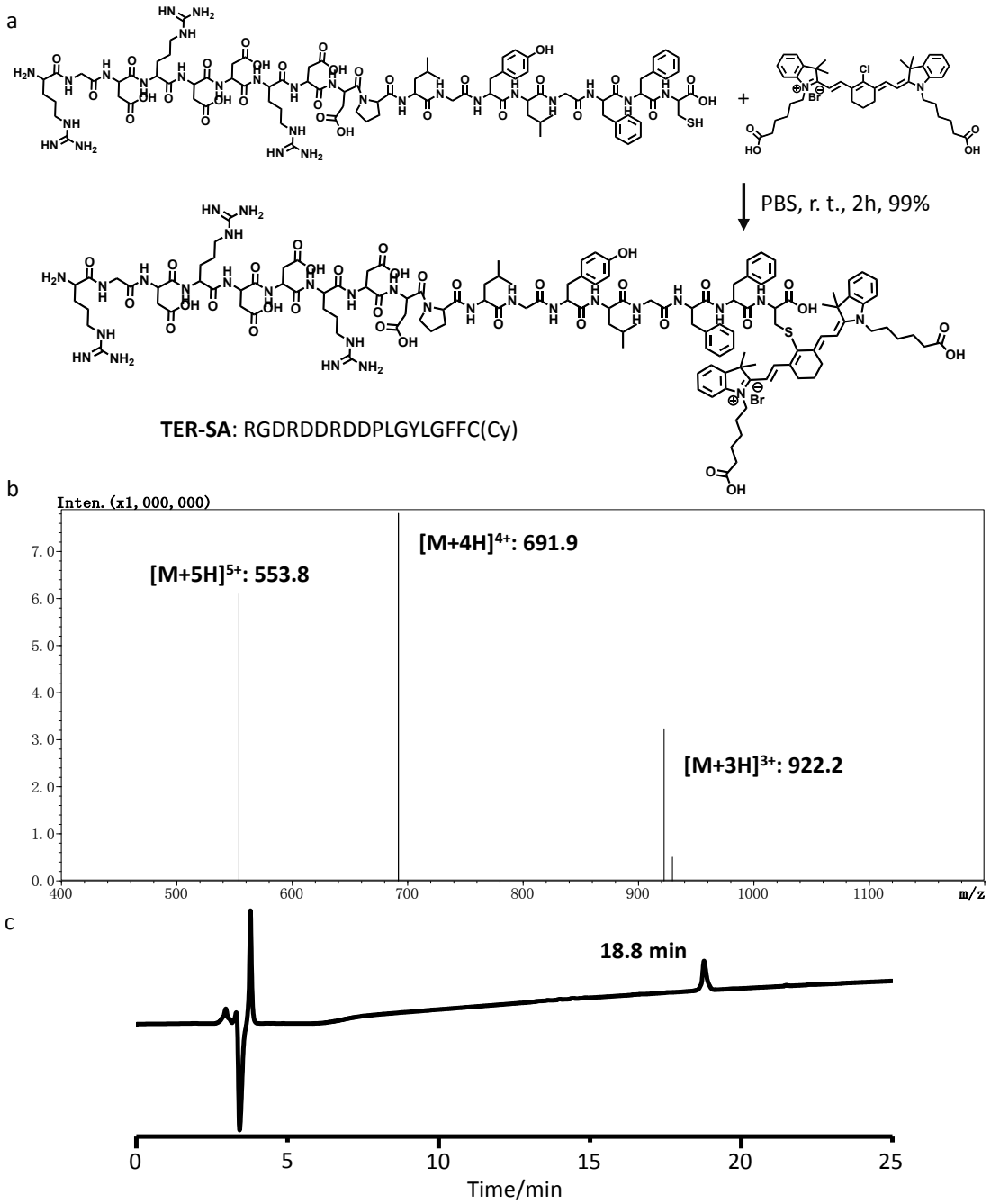

Scheme S2. (a) The structure of **TER-SA**; (b) MS-ESI and (c) HPLC spectra of **TER-SA**. The method of HPLC spectra was as follows: solvent A, 0.1% trifluoroacetic in 100% water; solvent B, 0.1% trifluoroacetic in 100% acetonitrile; 0.01 min, 20% solvent B, 25 min, 80% solvent B.

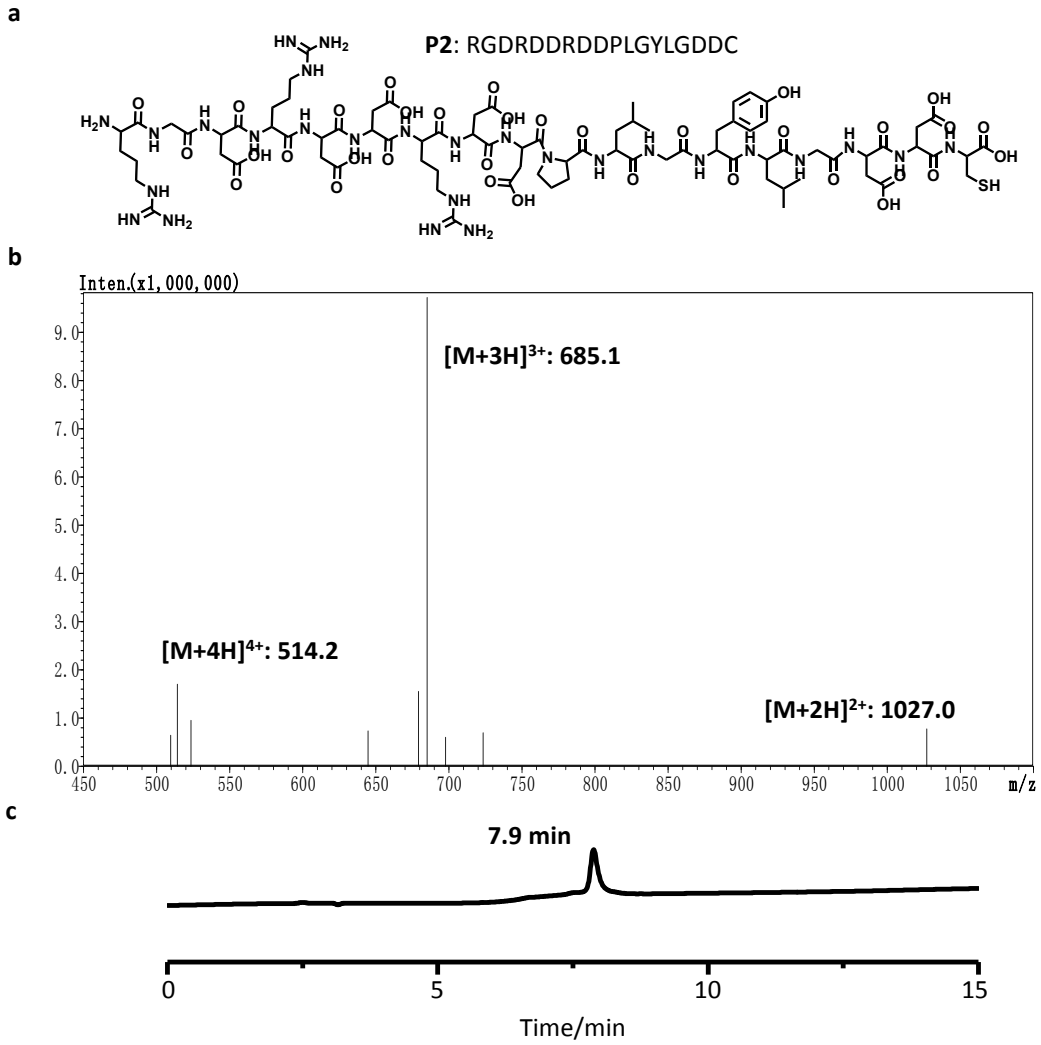

Scheme S3. (a) The structure of P2; (b) MS-ESI (c) and HPLC spectra of P2. The method of HPLC spectra was as follows: solvent A, 0.1% trifluoroacetic in 100% water; solvent B, 0.1% trifluoroacetic in 100% acetonitrile; 0.01 min, 25% solvent B, 15 min, 65% solvent B.

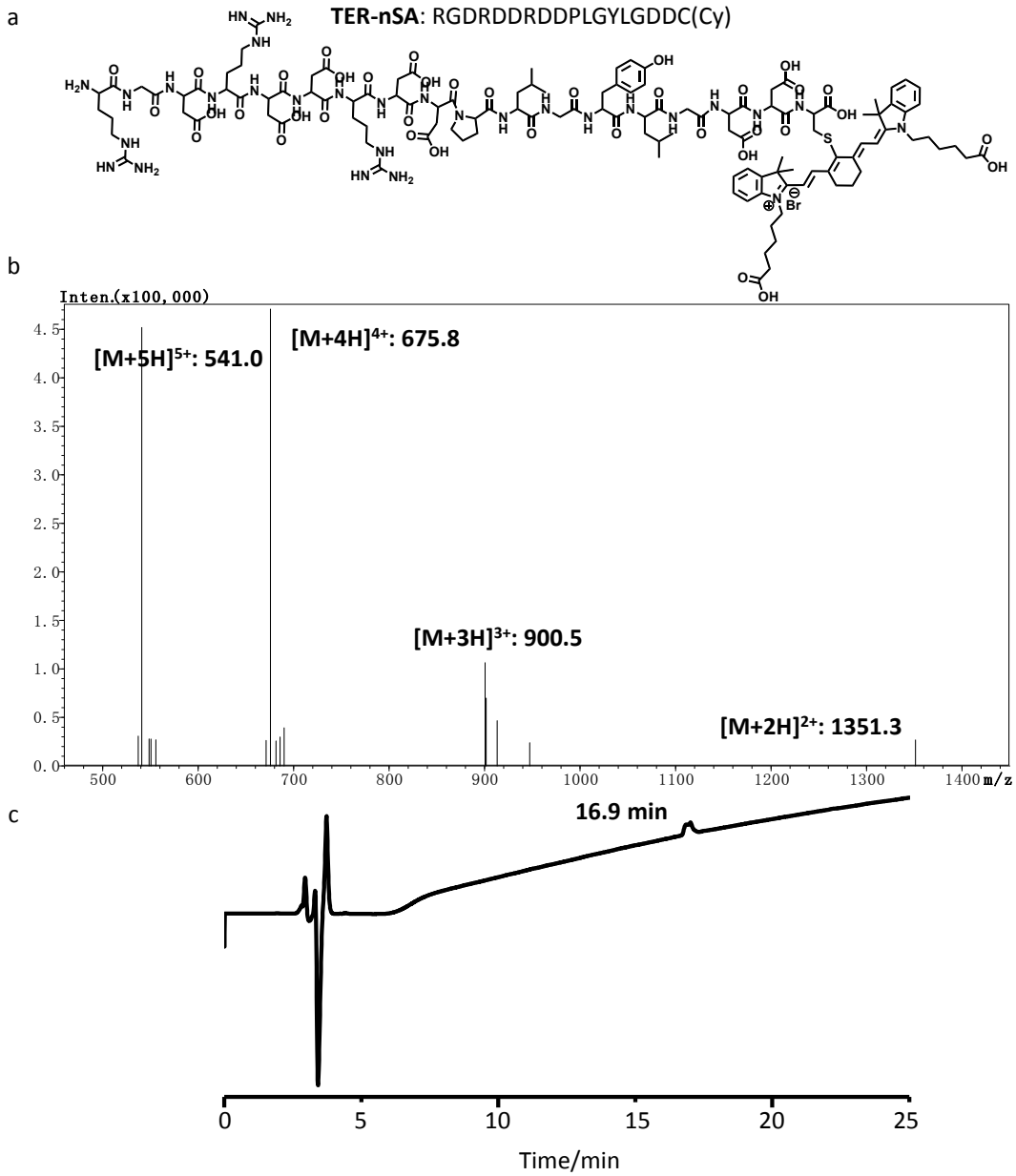

Scheme S4. (a) The structure of **TER-nSA**; (b) MS-ESI (c) and HPLC spectra of **TER-nSA**. The method of HPLC spectra was as follows: solvent A, 0.1% trifluoroacetic in 100% water; solvent B, 0.1% trifluoroacetic in 100% acetonitrile; 0.01 min, 20% solvent B, 25 min, 80% solvent B.

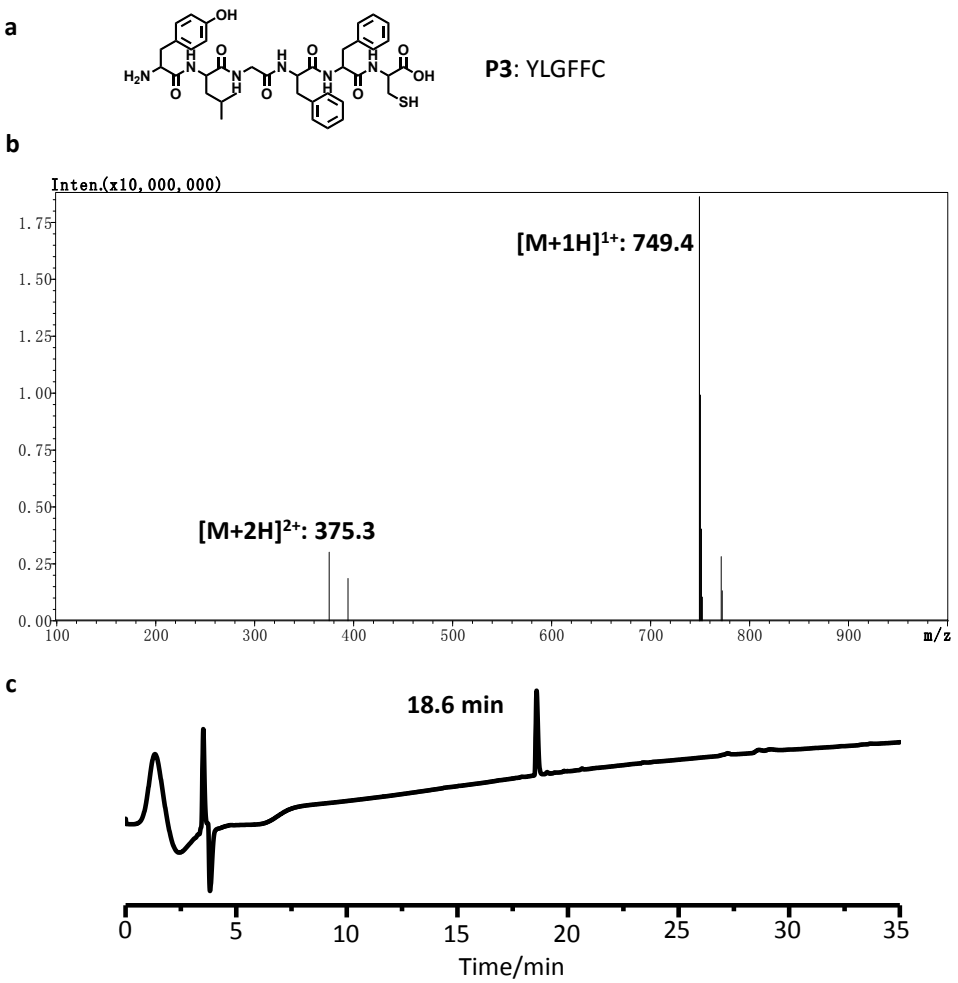

Scheme S5. (a) The structure of P3. (b) MS-ESI and (c) HPLC spectra of P3. The method of HPLC spectra was as follows: solvent A, 0.1% trifluoroacetic in 100% water; solvent B, 0.1% trifluoroacetic in 100% acetonitrile; 0.01 min, 10% solvent B, 35 min, 90% solvent B.

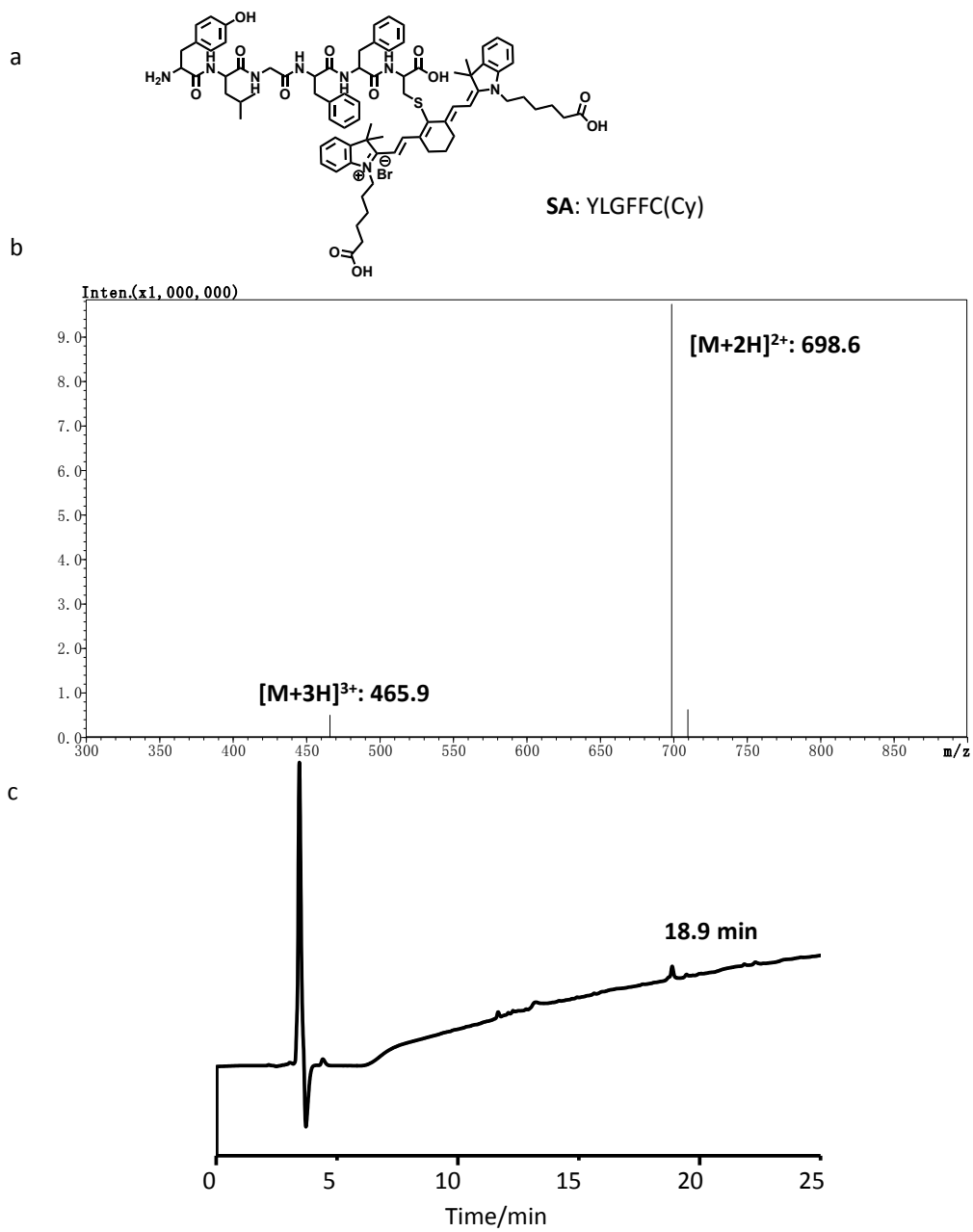

Scheme S6. (a) The structure of **SA**. (b) MS-ESI and (c) HPLC spectra of **SA**. The method of HPLC spectra was as follows: solvent A, 0.1% trifluoroacetic in 100% water; solvent B, 0.1% trifluoroacetic in 100% acetonitrile; 0.01 min, 20% solvent B, 25 min, 80% solvent B.

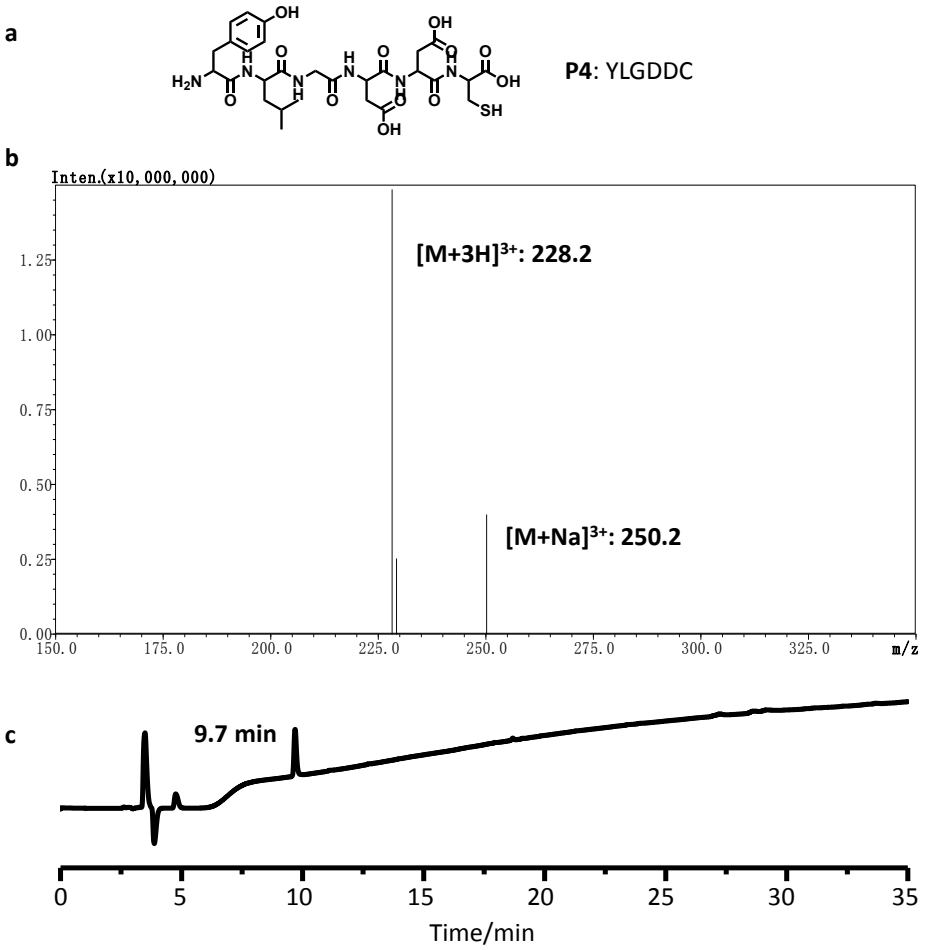

Scheme S7. (a) The structure of P4; (b) MS-ESI and (c) HPLC spectra of P4. The method of HPLC spectra was as follows: solvent A, 0.1% trifluoroacetic in 100% water; solvent B, 0.1% trifluoroacetic in 100% acetonitrile; 0.01 min, 10% solvent B, 35 min, 90% solvent B.

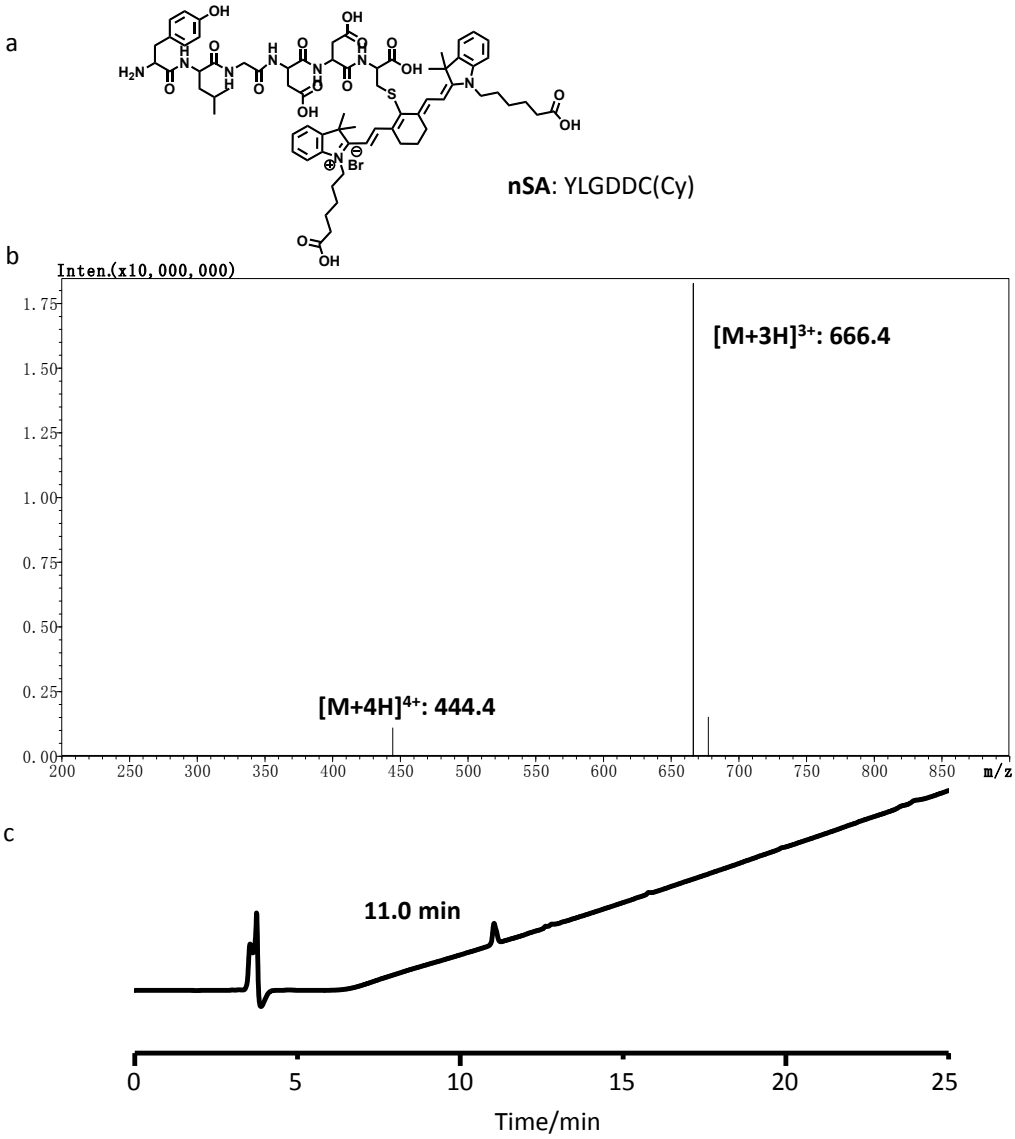

Scheme S8. (a) The structure of **nSA**; (b) MS-ESI and (c) HPLC spectra of **nSA**. The method of HPLC spectra was as follows: solvent A, 0.1% trifluoroacetic in 100% water; solvent B, 0.1% trifluoroacetic in 100% acetonitrile; 0.01 min, 10% solvent B, 25 min, 90% solvent B.

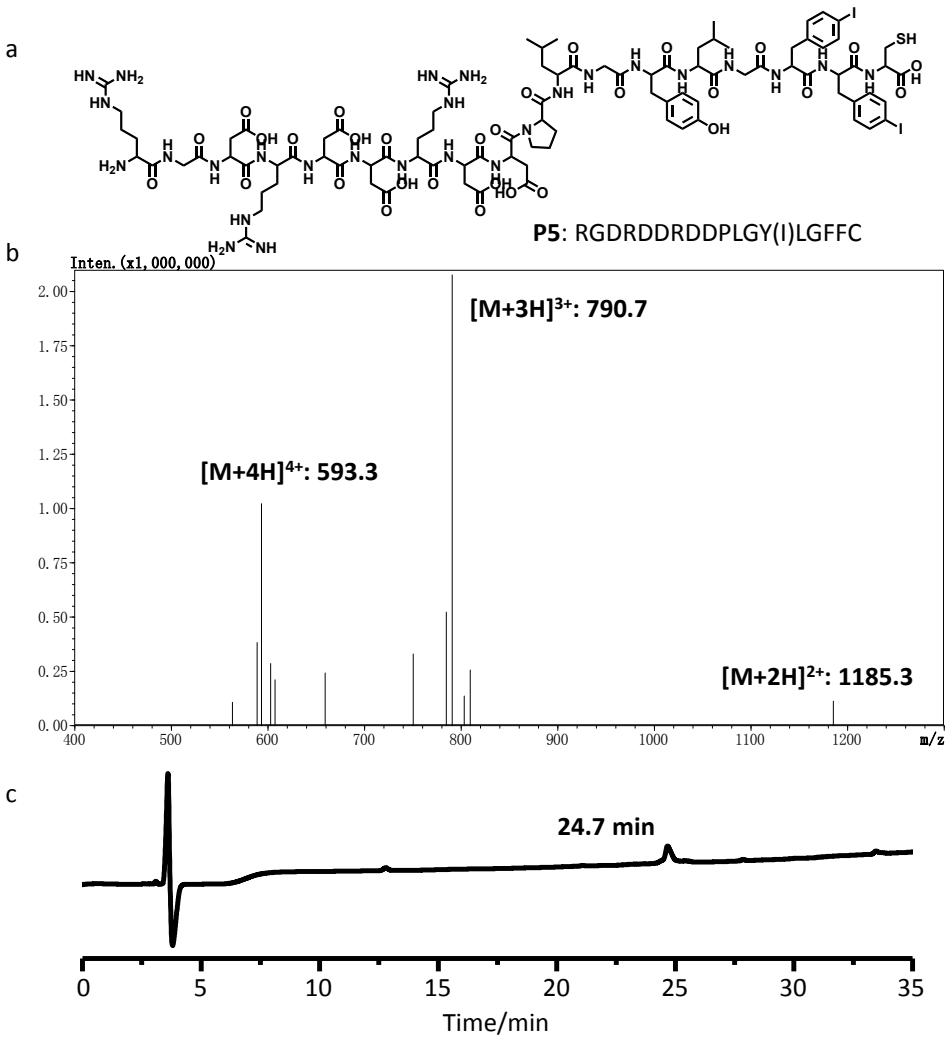

Scheme S9. (a) The structure of P5; (b) MS-ESI and (c) HPLC spectra of P5. The method of HPLC spectra was as follows: solvent A, 0.1% trifluoroacetic in 100% water; solvent B, 0.1% trifluoroacetic in 100% acetonitrile; 0.01 min, 15% solvent B, 35 min, 70% solvent B.

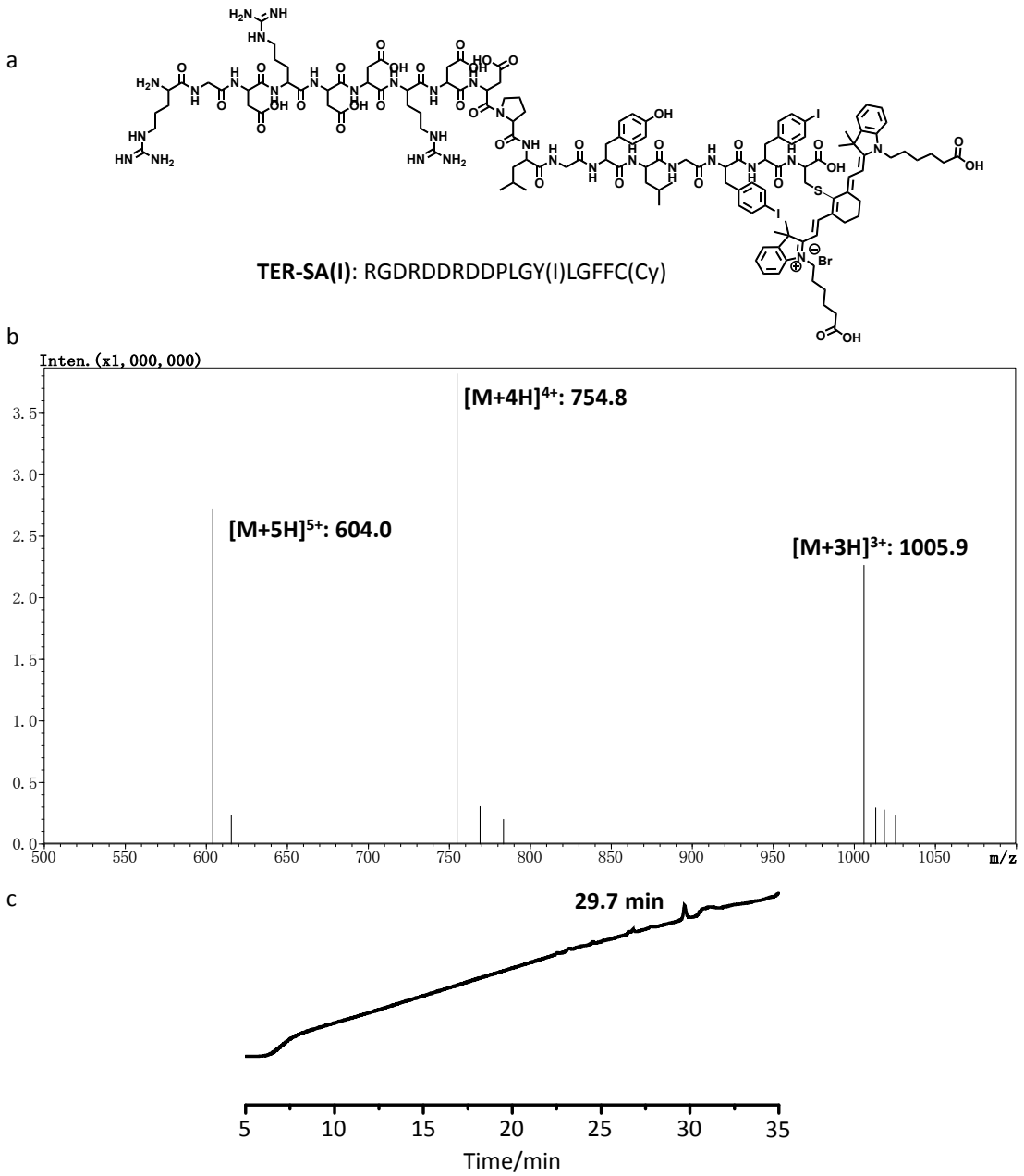

Scheme S10. (a) The structure of **TER-nSA(I)**; (b) MS-ESI and (c) HPLC spectra of **TER-nSA(I)**. The method of HPLC spectra was as follows: solvent A, 0.1% trifluoroacetic in 100% water; solvent B, 0.1% trifluoroacetic in 100% acetonitrile; 0.01 min, 15% solvent B, 35 min, 70% solvent B.

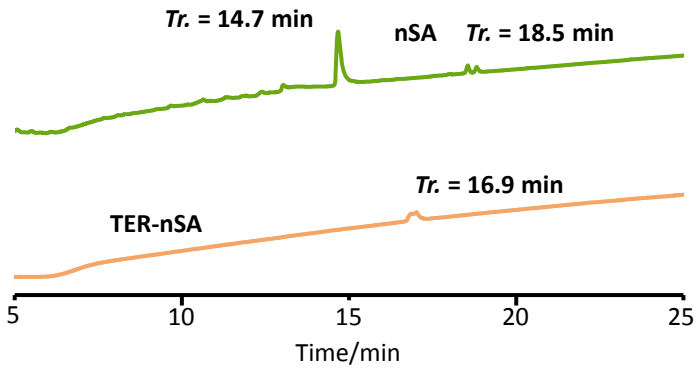

Figure S1. The HPLC analysis of **TER-nSA** (500 μM) and co-incubation of **TER-nSA** (500 μM) and MMP-2/9 (15 μg/ml).

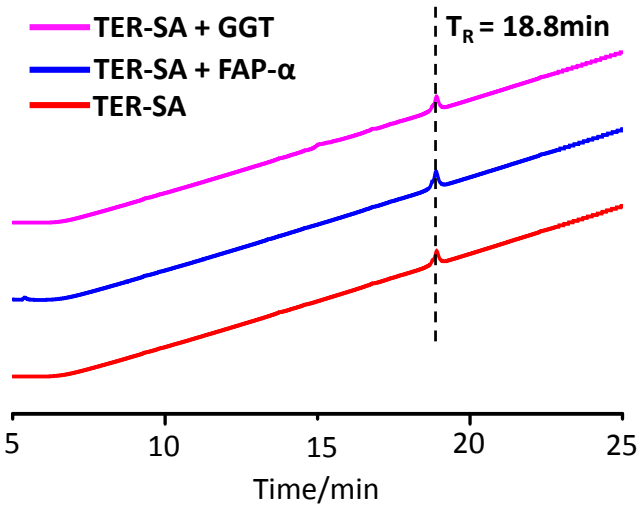

Figure S2. The HPLC analysis of TER-SA (500 μM), co-incubation of TER-SA (500 μM) and FAP-α (Fibroblast Activation Protein-α, 15 μg/ml) and co-incubation of TER-SA (500 μM) and GGT (Gamma-Glutamyl Transpeptidase, 10 U/ml).

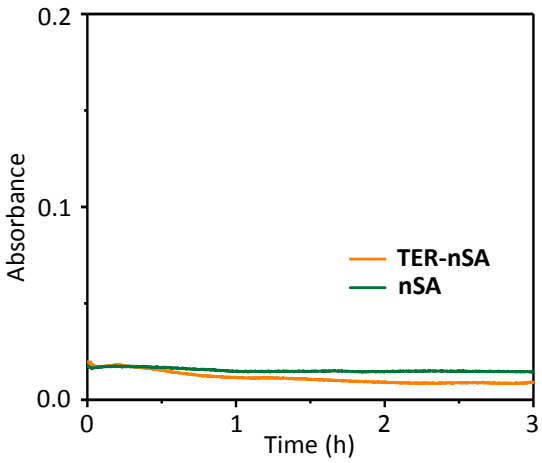

Figure S3. Turbidity response for **TER-nSA** (50 μM) and **nSA** (50 μM) for 3 h at 25 ℃.

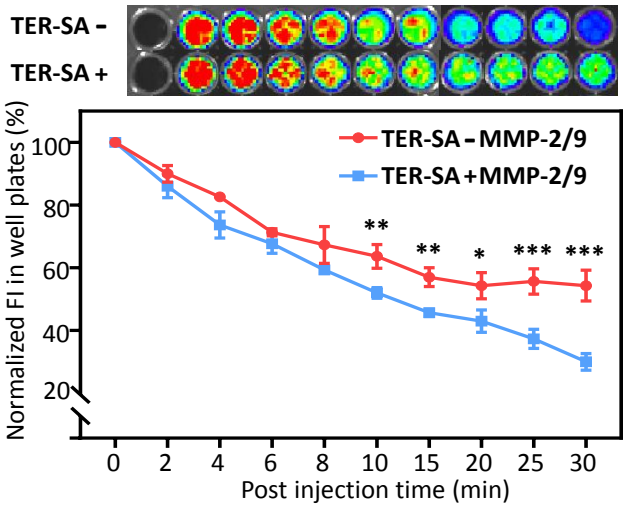

Figure S4. Photostability evaluation of **TER-SA** and **TER-SA + MMP-2/9** under near infrared laser irradiation. **TER-SA** (50 μM) were dissolved TES buffer (0.36 mM $CaCl_2$, pH 7.4) for 0, 2, 4, 6, 8, 10, 15, 20, 25 and 30 min. Asterisks (*) denote the statistical significance: * $p < 0.05$, ** $p < 0.01$, *** $p < 0.001$, p values were performed with one-way ANOVA followed by post hoc Tukey's test. All experiments were repeated 3 times. Data were expressed as mean ± SD (n = 3).

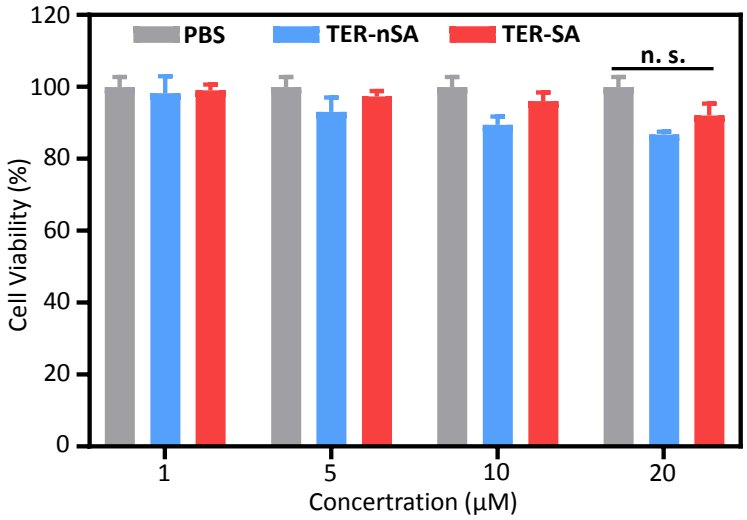

Figure S5. Cell viability assay of 786-O cells treated with a series of concentrations of PBS, **TER-nSA** and **TER-SA** for 24 h. Asterisks (*) denote the statistical significance: n.s. means no significance, p values were performed with one-way ANOVA followed by post hoc Tukey's test. Data were expressed as mean ± SD (n = 3).

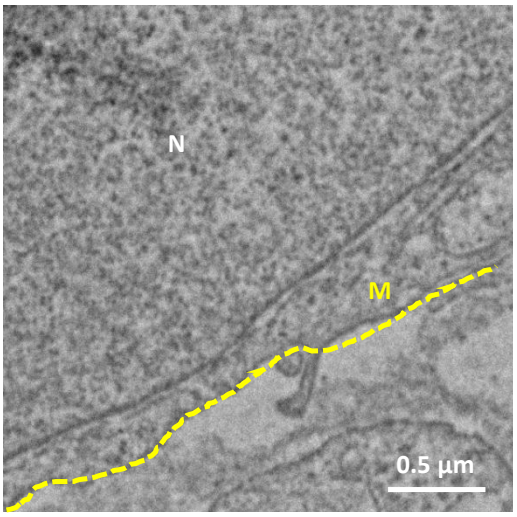

Figure S6. The TEM images of tumor tissue slices of 786-O xenografted mice i.v. injected with PBS at 6 h. M labels the cytomembrane of the 786-O cell. N labels the nucleus of the 786-O cell. Scale bar = 0.5 μm.

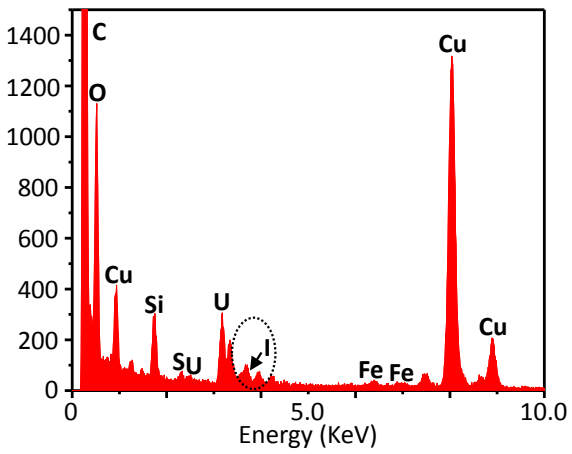

Figure S7. Energy dispersive spectroscopy (EDS) scanning of the elemental distribution of the nanofibers in ultrathin sections of tumors treated with TER-SA(I).

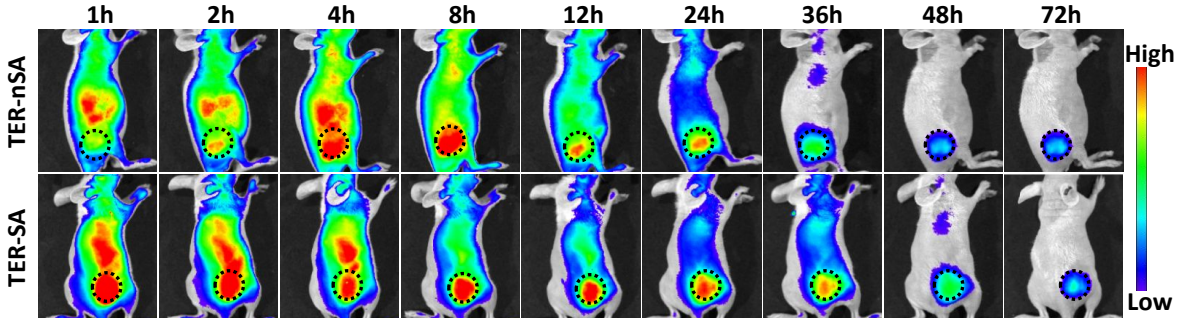

Figure S8. Representative NIR fluorescence images of 786-O xenograft mice after intravenous administration with with **TER-nSA** (3 mg/kg, n = 3) and **TER-SA** (3 mg/kg, n = 3). Images were acquired at 1 h, 2 h, 4 h, 8h, 12 h, 12h, 24 h, 36h, 48h and 72 h post injection (p.i.). The black circles marked the same size of the tumor region.

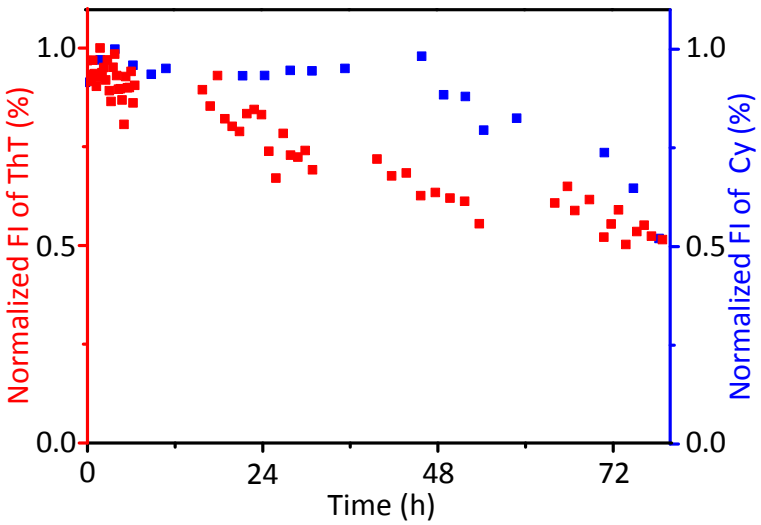

Figure S9. The normalized fluorescence intensity of Cy for 80 h in nanofibers formed by SA (50 μM) (blue) and normalized fluorescence intensity of ThT (10 μM) after co-incubated with the nanofibers formed by SA (50 μM) for 80 h (red).

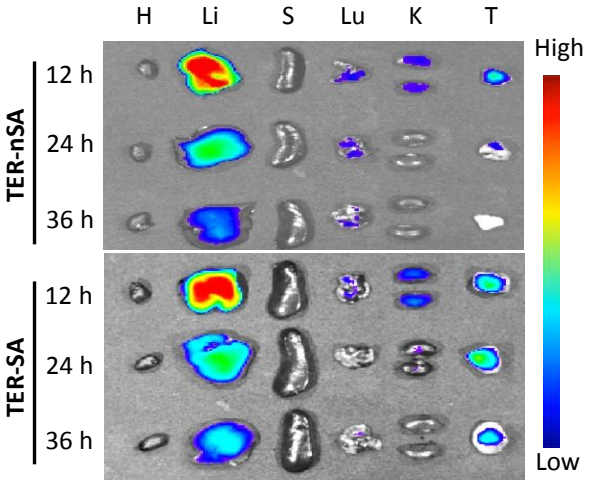

Figure S10. *Ex vivo* NIR fluorescence images of tumor and major organs collected at 12, 24 and 36 h after intravenous injection of **TER-nSA** and **TER-SA**, respectively (3 mg/kg, n = 3). H (heart), Li (liver), S (spleen), Lu (lung), K (kidney), T (tumor).

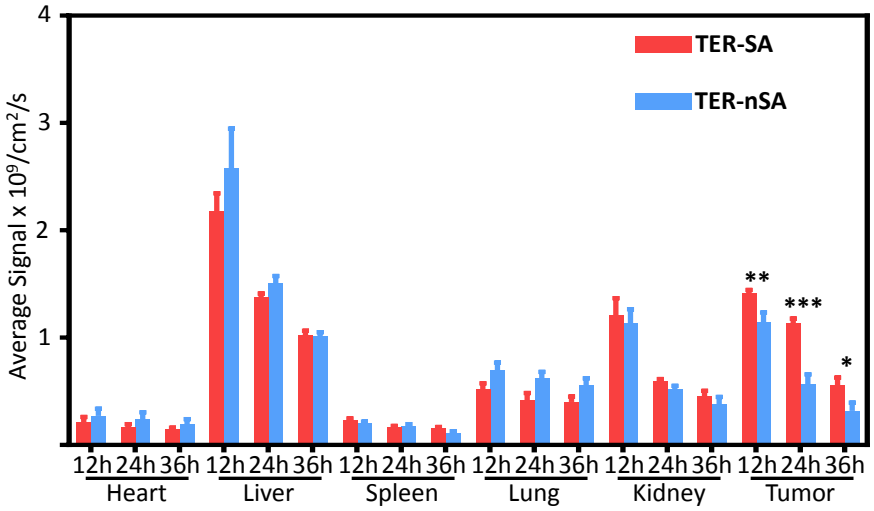

Figure S11. Quantitative analysis for the biodistribution in major organs in panel Figure S8. Asterisks (*) denote the statistical significance: * $p < 0.05$, ** $p < 0.01$, *** $p < 0.001$, p values were performed with one-way ANOVA followed by post hoc Tukey's test. All experiments were repeated 3 times. Data were expressed as mean ± SD (n = 3).

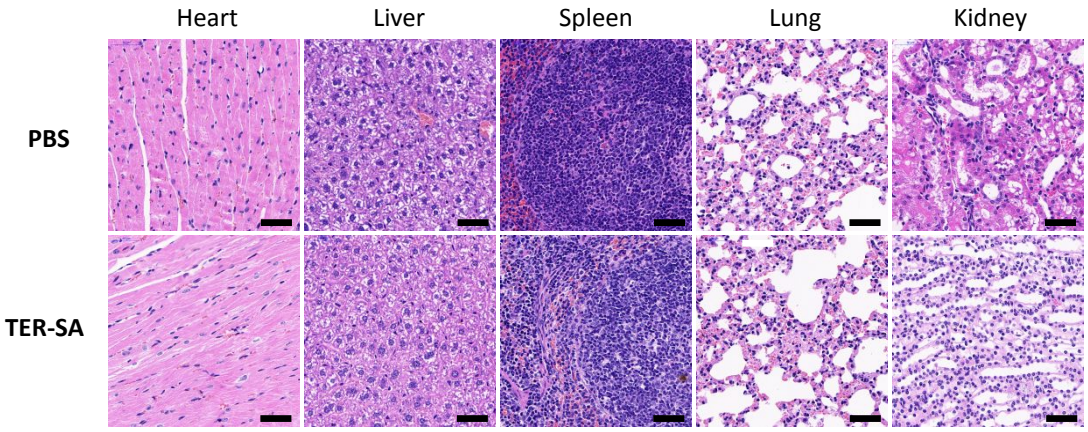

Figure S12. Histology evaluation of the major organs (heart, liver, spleen, lung, and kidney) collected from the **PBS** treated group and **TER-SA** treated group. Scale bar = 50 μm.

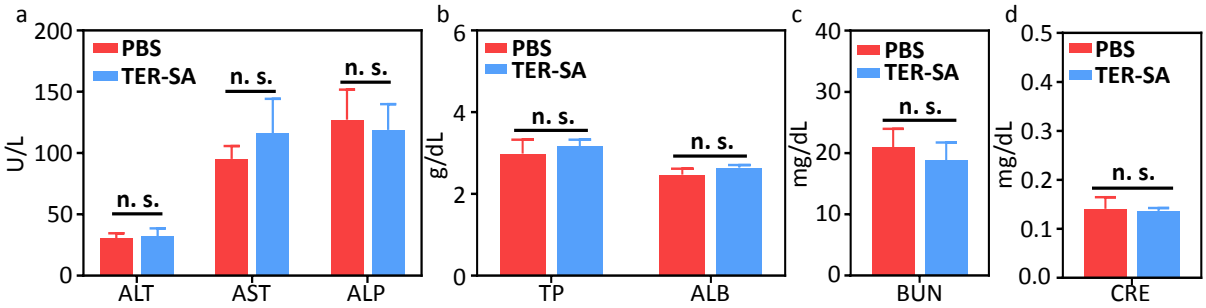

Figure S13. Blood biochemistry data of the nude mice which were treated with TER-SA (3.5 mg/kg). The PBS group was nude mice which were treated with PBS. (a) Major indicators of liver function, alanine aminotransferase (ALT), aspartate aminotransferase (AST) and alkaline phosphatase (ALP) levels. (b) Total Protein (TP) and albumin (ALB) levels. (c) The blood urea nitrogen (BUN) and (d) creatinine (CRE) levels, important indicators of kidney function. Asterisks (*) denote the statistical significance: n. s. means no significance, p values were performed with one-way ANOVA followed by post hoc Tukey's test. Data were expressed as mean ± SD (n = 5).

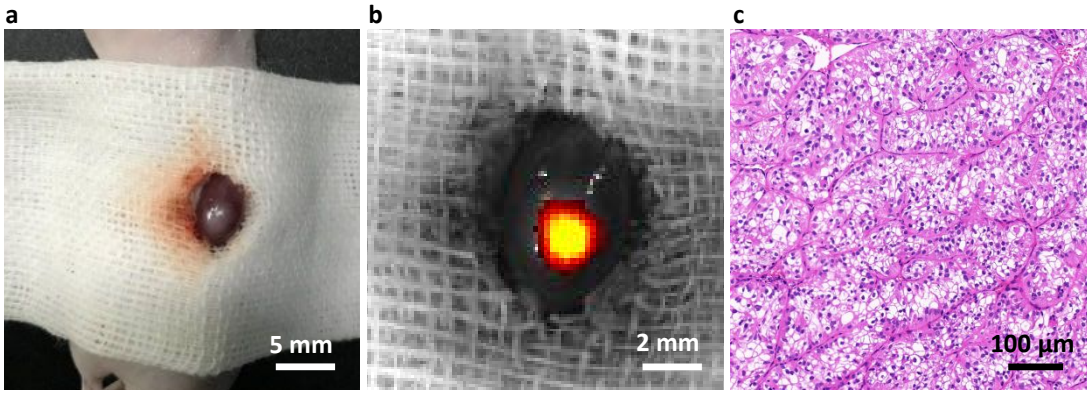

Figure S14. Images of the orthotopic RCC xenograft nude mice model and H&E staining result of the orthotopic tumor tissue. (a) BF images of the orthotopic RCC xenograft nude mice. Scale bar = 5 mm; (b) Bio-luminescence images of successfully constructed orthotopic tumor. Scale bar = 2 mm; (c) H&E staining result of the successfully constructed orthotopic tumor tissue. Scale bar = 100 μm.

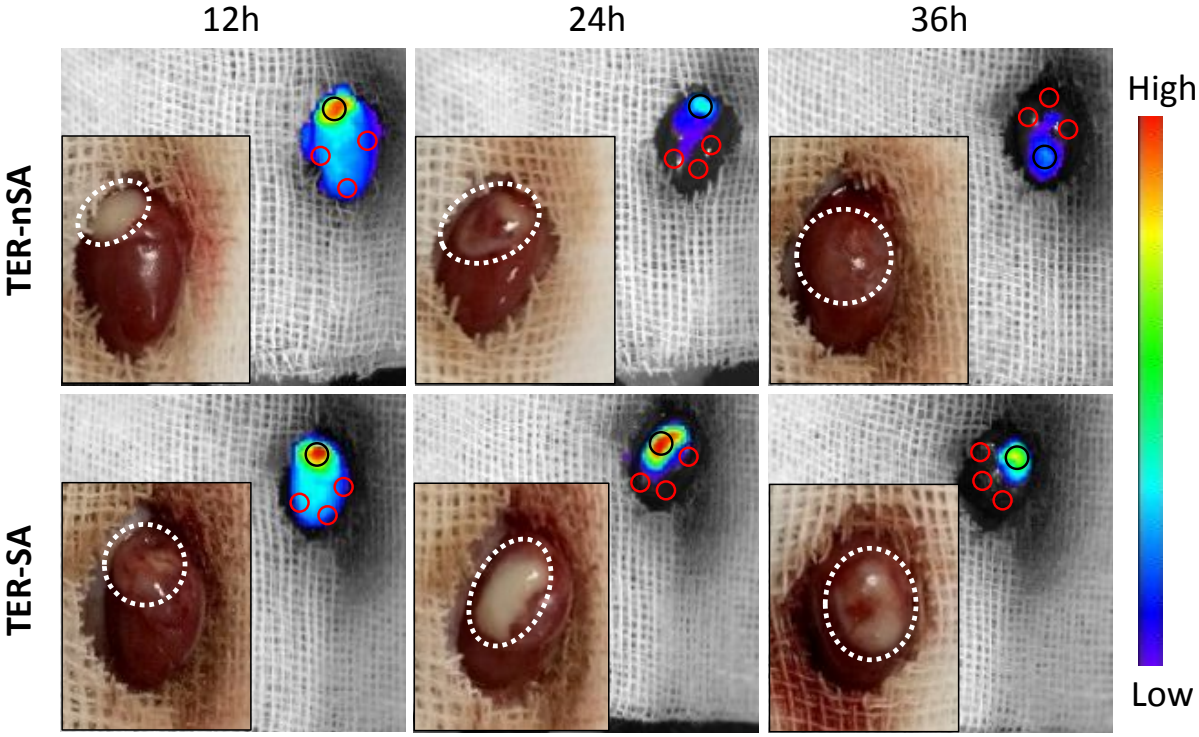

Figure S15. Representative NIR fluorescence images of TER-SA and TER-nSA (3 mg/kg, n = 3) on the orthotopic 786-O RCC xenograft mice after intravenous administration. Images were acquired at 24 h, 36 h and 48 h post injection. The region of tumor tissue which was used for calculating S/N ratio was labeled with black circle; and the region of normal tissue which was used for calculating S/N ratio was labeled with red circle. Scale bar = 2 mm.

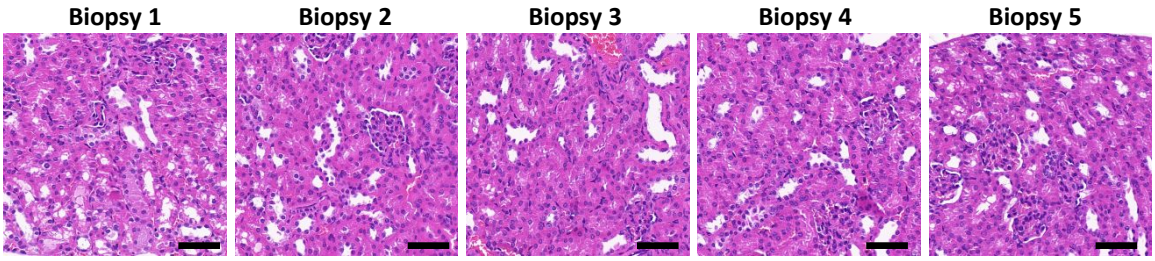

Figure S16. Images of the H&E-stained tissue section obtained at surgical margin were shown. Scale bar = 50 μm.

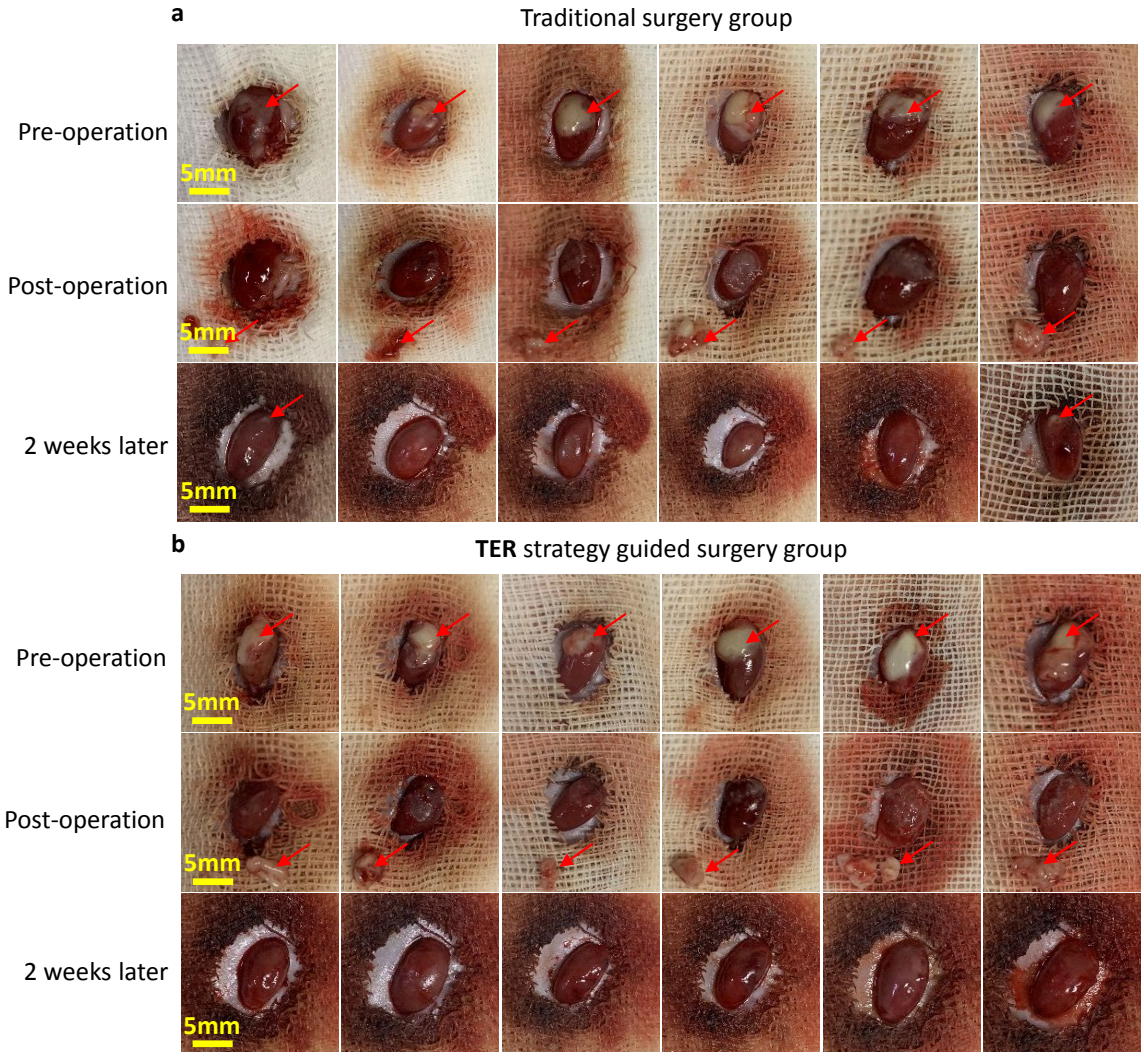

Figure S17. The recurrence result of (a) traditional surgery group and (b) **TER** strategy guided surgery group. Scale bar = 5 mm.

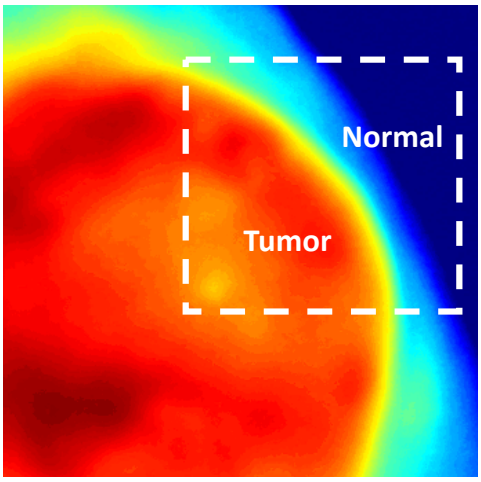

Figure S18. Representative images which showed the boundaries between tumor regions and surrounding normal tissues.

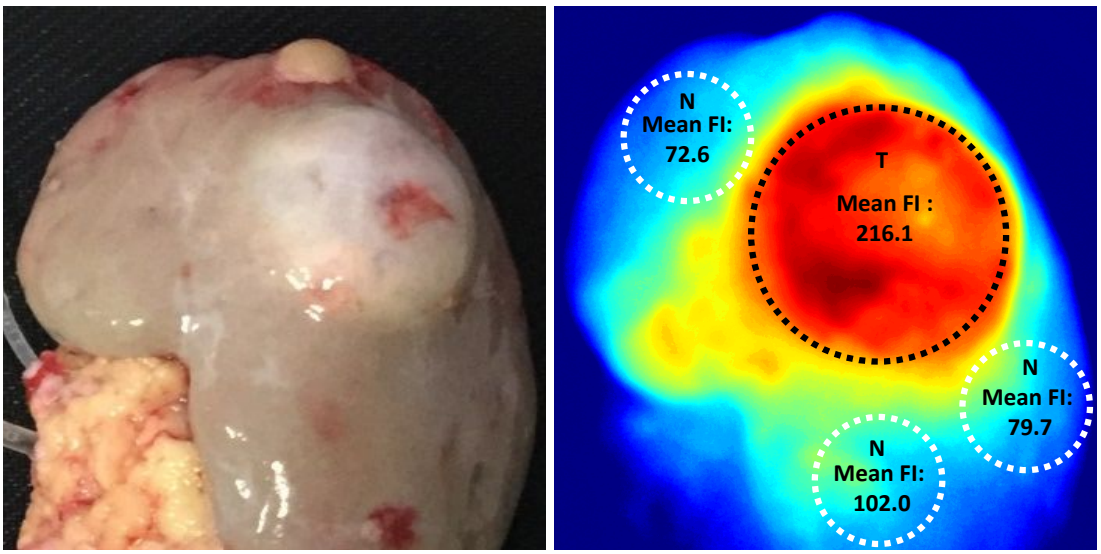

Figure S19. Representative images of morphological image and fluorescence image of the tumor-bearing kidney. The region of tumor tissue which was used for calculating S/N ratio was labeled with black circle (tumor); and the region of normal tissue which was used for calculating S/N ratio was labeled with white circle (normal).

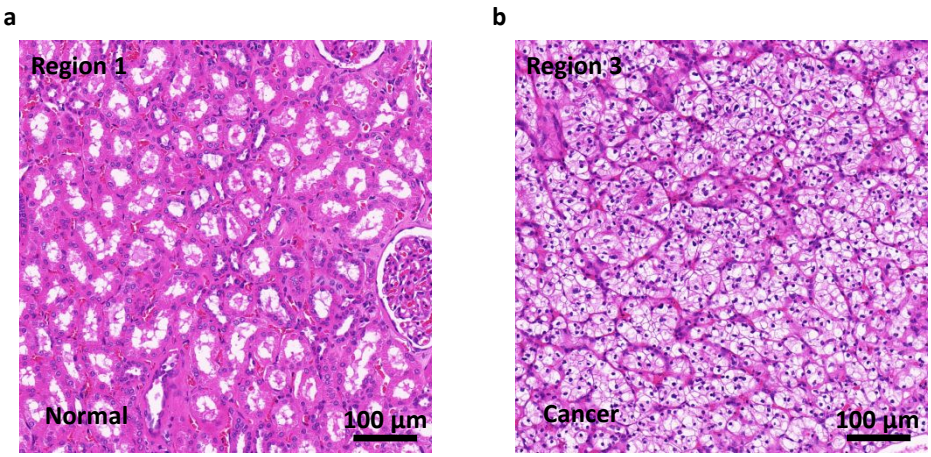

Figure S20. Images of the H&E-stained tissue section obtained at region 1 and 3 were shown. (a) Region 1 presented a histologic composition of normal tissue, (b) region 3 presented a histologic composition of normal tissue. The diagnosis was confirmed by pathological analysis. Scale bar = 100 µm.